



d-Wave superconductivity from correlated-hopping interactions determined by angle-resolved photoemission spectroscopy

César G. Galván^a, Luis A. Pérez^b, Chumin Wang^{a,*}

^a Instituto de Investigaciones en Materiales, Universidad Nacional Autónoma de México, A.P. 70-360, 04510, D.F., México, Mexico

^b Instituto de Física, Universidad Nacional Autónoma de México, A.P. 20-364, 01000, D.F., México, Mexico

ARTICLE INFO

Article history:

Received 6 December 2011

Received in revised form 23 February 2012

Accepted 26 February 2012

Available online 3 March 2012

Communicated by R. Wu

Keywords:

d-Wave superconductivity

Hubbard model

ARPES

ABSTRACT

Starting from a generalized Hubbard model with correlated-hopping interactions, we solve numerically two coupled integral equations within the Bardeen–Cooper–Schrieffer formalism, in order to study the doping effects on the critical temperature (T_c), *d*-wave superconducting gap, and the electronic specific heat. Within the mean-field approximation, we determine the single- and correlated-electron-hopping parameters for $\text{La}_{2-x}\text{Sr}_x\text{CuO}_4$ by using angle-resolved photoemission spectroscopy data. The resulting parametrized Hubbard model is able to explain the experimental T_c variation with the doping level (x). Moreover, the observed power-law behavior of the superconducting specific heat is reproduced by this correlated-hopping Hubbard model without adjustable parameters.

© 2012 Elsevier B.V. All rights reserved.

1. Introduction

The microscopic theory developed in 1957 by J. Bardeen, L.N. Cooper and J.R. Schrieffer (BCS) [1] was successful in explaining the main features of metallic superconductors. In the last two decades, the observation of *d*-symmetry pairing in ceramic superconductors has motivated the research of models beyond the standard BCS theory to include anisotropic superconducting gaps. Experimental evidence such as a corner superconducting quantum interference device (SQUID) made of a conventional superconductor and two orthogonally oriented plane faces of a single ceramic superconductor [2], as well as the spontaneous generation of a half-flux quantum at the meeting point of Josephson coupled superconducting crystals [3], strongly suggests a *d*-wave order parameter in many ceramic superconductors. In these materials, the charge carriers are confined to move mainly on the CuO_2 planes. This quasi-two-dimensional behavior could be essential to understand their superconducting properties. Hence, three-band Hubbard models have been proposed to describe the dynamics of the carriers on the CuO_2 planes [4], and the electronic states close to the Fermi energy can be reasonably well described by a single-band tight-binding model on a square lattice with a second-neighbor hopping [5]. Furthermore, it has been shown that the second-neighbor correlated-hopping interactions could lead to *d*-wave superconducting ground states [6]. Even in this single-band generalized Hubbard model there are several pa-

rameters that should be determined. In this Letter, we propose a new way to find out single- and correlated-electron-hopping parameters through the angle-resolved photoemission spectroscopy (ARPES) within the mean-field approximation. In particular, we applied this method to $\text{La}_{2-x}\text{Sr}_x\text{CuO}_4$ systems and found a good agreement between the theoretical results and experimental data of the critical temperature (T_c) as well as the electronic specific heat. It is worth mentioning that the tight-binding parameters are usually determined by fitting ARPES data as done in Refs. [7–9], but none of them has further studied T_c neither specific heat.

2. The model

Let us start from a single-band square-lattice Hubbard model with on-site Coulombic interaction (U), first- (Δt) and second-neighbor (Δt_3) correlated-hopping interactions. Certainly, Δt and Δt_3 are always present in real materials and in spite of having small strengths, they are essential in the determination of the superconducting symmetry. The corresponding Hamiltonian can be written as

$$\begin{aligned} \hat{H} = & \varepsilon_0 \sum_{i,\sigma} \hat{c}_{i,\sigma}^+ \hat{c}_{i,\sigma} + t \sum_{\langle i,j \rangle} \hat{c}_{i,\sigma}^+ \hat{c}_{j,\sigma} + t' \sum_{\langle\langle i,j \rangle\rangle} \hat{c}_{i,\sigma}^+ \hat{c}_{j,\sigma} \\ & + U \sum_i \hat{n}_{i,\uparrow} \hat{n}_{i,\downarrow} + \Delta t \sum_{\langle i,j \rangle} \hat{c}_{i,\sigma}^+ \hat{c}_{j,\sigma} (\hat{n}_{i,-\sigma} + \hat{n}_{j,-\sigma}) \\ & + \Delta t_3 \sum_{\langle\langle i,j \rangle\rangle} \hat{c}_{i,\sigma}^+ \hat{c}_{j,\sigma} \hat{n}_l, \end{aligned} \quad (1)$$

* Corresponding author.

E-mail address: chumin@unam.mx (C. Wang).

where $\hat{c}_{i,\sigma}^\dagger$ ($\hat{c}_{i,\sigma}$) is the creation (annihilation) operator with spin $\sigma = \downarrow$ or \uparrow at site i , $\hat{n}_{i,\sigma} = \hat{c}_{i,\sigma}^\dagger \hat{c}_{i,\sigma}$, $\hat{n}_i = \hat{n}_{i,\uparrow} + \hat{n}_{i,\downarrow}$, $\langle i, j \rangle$ denote respectively first- and second-neighbor sites. This model can lead to s - and d -wave superconducting ground states without negative U [6]. Performing a Fourier transform, this Hamiltonian in the momentum space becomes

$$\begin{aligned} \hat{H} = & \sum_{\mathbf{k},\sigma} \varepsilon(\mathbf{k}) \hat{c}_{\mathbf{k},\sigma}^\dagger \hat{c}_{\mathbf{k},\sigma} \\ & + \frac{1}{N_s} \sum_{\mathbf{k},\mathbf{k}',\mathbf{q}} V_{\mathbf{k},\mathbf{k}',\mathbf{q}} \hat{c}_{\mathbf{k}+\mathbf{q},\uparrow}^\dagger \hat{c}_{-\mathbf{k}'+\mathbf{q},\downarrow}^\dagger \hat{c}_{-\mathbf{k}'+\mathbf{q},\downarrow} \hat{c}_{\mathbf{k}+\mathbf{q},\uparrow} \\ & + \frac{1}{N_s} \sum_{\mathbf{k},\mathbf{k}',\mathbf{q},\sigma} W_{\mathbf{k},\mathbf{k}',\mathbf{q}} \hat{c}_{\mathbf{k}+\mathbf{q},\sigma}^\dagger \hat{c}_{-\mathbf{k}'+\mathbf{q},\sigma}^\dagger \hat{c}_{-\mathbf{k}'+\mathbf{q},\sigma} \hat{c}_{\mathbf{k}+\mathbf{q},\sigma}, \end{aligned} \quad (2)$$

where N_s is the total number of sites,

$$\varepsilon(\mathbf{k}) = \varepsilon_0 + 2t[\cos(k_x a) + \cos(k_y a)] + 4t' \cos(k_x a) \cos(k_y a), \quad (3)$$

$$\begin{aligned} V_{\mathbf{k},\mathbf{k}',\mathbf{q}} = & U + \Delta t [\beta(\mathbf{q} + \mathbf{k}) + \beta(\mathbf{q} - \mathbf{k}) \\ & + \beta(\mathbf{q} + \mathbf{k}') + \beta(\mathbf{q} - \mathbf{k}')] \\ & + \Delta t_3 [\gamma(\mathbf{q} + \mathbf{k}, \mathbf{q} + \mathbf{k}') + \gamma(\mathbf{q} - \mathbf{k}, \mathbf{q} - \mathbf{k}')], \end{aligned} \quad (4)$$

and

$$W_{\mathbf{k},\mathbf{k}',\mathbf{q}} = \Delta t_3 \gamma(\mathbf{q} + \mathbf{k}, \mathbf{q} + \mathbf{k}'), \quad (5)$$

being

$$\beta(\mathbf{k}) = 2[\cos(k_x a) + \cos(k_y a)], \quad (6)$$

$$\gamma(\mathbf{k}, \mathbf{k}') = 4 \cos(k_x a) \cos(k'_x a) + 4 \cos(k'_y a) \cos(k_y a), \quad (7)$$

and $2\mathbf{q}$ is the wave vector of the pair center of mass. After a standard Hartree-Fock decoupling of the interaction terms with $\mathbf{q} \neq \mathbf{0}$ [10] applied to Eq. (2), the reduced Hamiltonian for $\mathbf{q} = \mathbf{0}$ is

$$\begin{aligned} \hat{H} = & \sum_{\mathbf{k},\sigma} \varepsilon_{MF}(\mathbf{k}) \hat{c}_{\mathbf{k},\sigma}^\dagger \hat{c}_{\mathbf{k},\sigma} + \frac{1}{N_s} \sum_{\mathbf{k},\mathbf{k}'} V_{\mathbf{k},\mathbf{k}',\mathbf{0}} \hat{c}_{\mathbf{k},\uparrow}^\dagger \hat{c}_{-\mathbf{k}',\downarrow}^\dagger \hat{c}_{-\mathbf{k}',\downarrow} \hat{c}_{\mathbf{k},\uparrow} \\ & + \frac{1}{N_s} \sum_{\mathbf{k},\mathbf{k}',\sigma} W_{\mathbf{k},\mathbf{k}',\mathbf{0}} \hat{c}_{\mathbf{k},\sigma}^\dagger \hat{c}_{-\mathbf{k}',\sigma}^\dagger \hat{c}_{-\mathbf{k}',\sigma} \hat{c}_{\mathbf{k},\sigma}, \end{aligned} \quad (8)$$

where the mean-field dispersion relation of an effective square lattice with a lattice parameter a is given by

$$\begin{aligned} \varepsilon_{MF}(\mathbf{k}) = & \varepsilon_{eff} + 2t_{eff}[\cos(k_x a) + \cos(k_y a)] \\ & + 4t'_{eff} \cos(k_x a) \cos(k_y a) \end{aligned} \quad (9)$$

where $\varepsilon_{eff} = \varepsilon_0 + nU/2$, $t_{eff} = t + n\Delta t$, and $t'_{eff} = t' + 2n\Delta t_3$.

3. Parameter determination from ARPES data

Recently, ARPES experiments have been able to determine the electronic dispersion relationship, as well as the anisotropy of superconducting gaps in cuprate superconductors [11]. In particular, such dispersion relationship around the Fermi energy for $\text{La}_{2-x}\text{Sr}_x\text{CuO}_4$ with different doping levels (x) has been measured by extrapolating the peaks of momentum distribution curves up to the Fermi energy (E_F) even when the spectral weight is suppressed in going toward E_F due to the presence of an energy gap or pseudogap [12]. In Figs. 1(a)–(e), the calculated Fermi surfaces (blue solid squares) for $x = 0.03, 0.07, 0.15, 0.22$ and 0.30 are respectively shown and compared with ARPES experimental data (red open circles). Furthermore, Figs. 1(a')–(e') illustrate the corresponding fitted dispersion relations (blue solid squares) along

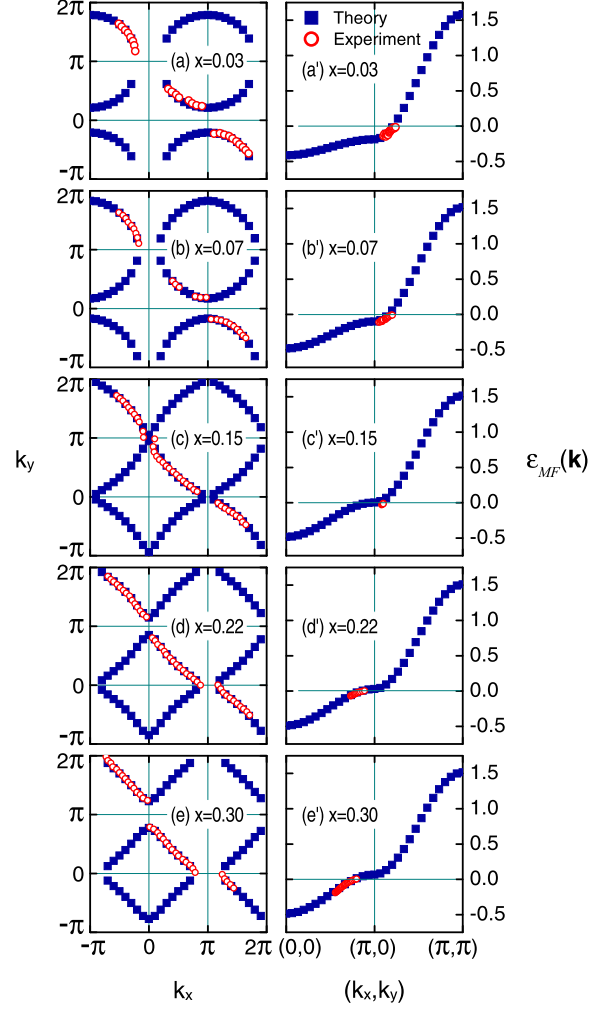


Fig. 1. (Color online.) ARPES data (red open circles) obtained from $\text{La}_{2-x}\text{Sr}_x\text{CuO}_4$ with different doping levels (x) indicated inside in comparison with the calculated dispersion relation (blue solid squares) at the Fermi energy (a)–(e) as well as along the $(0, 0)$ – $(\pi, 0)$ – (π, π) direction (a')–(e').

Table 1
Model parameters determined from ARPES data.

x	t_{eff} (eV)	t'_{eff} (eV)	ε_{eff} (eV)	n	Δt_3
0.03	−0.25	0.097	0.199	1.002	0.021
0.07	−0.25	0.077	0.209	0.938	0.021
0.15	−0.25	0.064	0.260	0.761	0.021
0.22	−0.25	0.060	0.268	0.716	0.021
0.30	−0.25	0.056	0.290	0.655	0.021

the $(0, 0)$ – $(\pi, 0)$ – (π, π) direction in comparison with experimental ones (red open circles). All the theoretical results of Fig. 1 have been obtained from Eq. (9) and the fitted value of ε_{eff} , t_{eff} , and t'_{eff} are summarized in Table 1, where the last two columns n and Δt_3 will be explained below. In particular, we have taken a constant value of $t_{eff} = -0.25$ eV as in Ref. [12], since only the relative magnitudes of t'_{eff}/t_{eff} and $\varepsilon_{eff}/t_{eff}$ are determined by ARPES data.

Once the effective hopping and self-energy parameters are obtained, the electronic density of states (DOS) can be calculated from [13]

$$\text{DOS}(E) = -\frac{1}{\pi} \lim_{\eta \rightarrow 0^+} \text{Im} \left[\sum_{\mathbf{k}} \frac{1}{E - \varepsilon_{MF}(\mathbf{k}) + i\eta} \right] \quad (10)$$

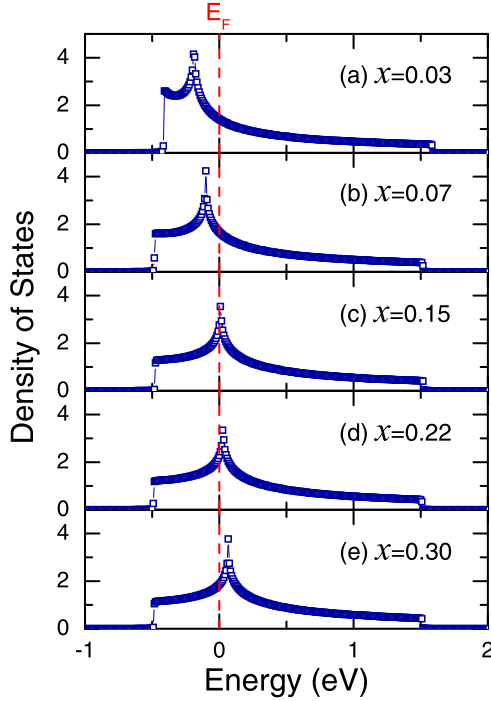


Fig. 2. (Color online.) Electronic density of states (DOS) for $x = 0.03, 0.07, 0.15, 0.22,$ and 0.30 corresponding to the mean-field dispersion relation (9) with the effective parameters shown in Table 1.

where $\varepsilon_{MF}(\mathbf{k})$ is the mean-field dispersion relation given by Eq. (9). The $DOS(E)$ for $x = 0.03, 0.07, 0.15, 0.22,$ and 0.30 are respectively shown in Figs. 2(a)–(e). Notice that for $x = 0.15$, the Fermi level (E_F) coincides with the van Hove singularity and then, the critical temperature is expected to be a maximum, according to the BCS theory [1]. By integrating $DOS(E)$ up to E_F we obtain the electronic density (n), whose numerical values for samples with different doping levels are listed in Table 1, where we observe an increase of the hole concentration from a half-filling electronic band as x grows.

4. Coupled integral equations

Applying the BCS formalism to Eq. (2), we find the following two coupled integral equations [6,14], which determine the d -wave superconducting gap [$\Delta(\mathbf{k})$] and the chemical potential (μ) for a given temperature (T) and electron density (n),

$$\Delta(\mathbf{k}) = -\frac{1}{2N_s} \sum_{\mathbf{k}'} \frac{V_{\mathbf{k},\mathbf{k}',\mathbf{0}} \Delta(\mathbf{k}')}{E(\mathbf{k}')} \tanh\left(\frac{E(\mathbf{k}')}{2k_B T}\right) \quad (11)$$

and

$$n - 1 = -\frac{1}{N_s} \sum_{\mathbf{k}'} \frac{\varepsilon_{MF}(\mathbf{k}') - \mu}{E(\mathbf{k}')} \tanh\left(\frac{E(\mathbf{k}')}{2k_B T}\right), \quad (12)$$

where the single-particle excitation energy is given by

$$E(\mathbf{k}) = \sqrt{(\varepsilon_{MF}(\mathbf{k}) - \mu)^2 + \Delta^2(\mathbf{k})}, \quad (13)$$

and $\Delta(\mathbf{k}) = \Delta_d[\cos(k_x a) - \cos(k_y a)]$. Eq. (11) can be rewritten as [6]

$$1 = \frac{4\Delta t_3 a^2}{8\pi^2} \int_{-\pi/a}^{\pi/a} \int_{-\pi/a}^{\pi/a} dk_x dk_y \frac{[\cos(k_x a) - \cos(k_y a)]^2}{E(\mathbf{k})} \times \tanh\left(\frac{E(\mathbf{k})}{2k_B T}\right), \quad (14)$$

where the double integral is always positive and then $\Delta t_3 > 0$ has a key participation in the formation of d -wave superconducting state within this model, in spite of its relative small strength.

The T_c can be obtained from Eq. (14) by taking $\Delta_d(T_c) = 0$ in Eq. (13). For $\text{La}_{2-x}\text{Sr}_x\text{CuO}_4$, we chose the maximum $T_c = 41$ K at $x = 0.15$ from T. Yoshida et al. [12] to determine the value of Δt_3 giving 0.021 eV. In Fig. 3, the calculated T_c (solid triangles) as a function of the Sr concentration (x) is shown and compared with experimental data from N. Momono et al. [15] (open circles) and from T. Yoshida et al. [12] (open squares). Observe that the Fermi energy at the van Hove singularity (see Fig. 2) seems to be a crucial criterion for the determination of maximum T_c , in accordance with the BCS theory [1,16]. The T_c as a function of n calculated by using the Hamiltonian parameters of Table 1 for $x = 0.15$ (solid squares) and $x = 0.22$ (solid circles) is illustrated in the inset of Fig. 3, where the corresponding values of x are indicated by dashed lines.

5. Specific heat results

One of the physical quantities that yields information about the symmetry of superconducting states is the electronic specific heat (C_{el}), which is given by [16]

$$C_{el} = \frac{2k_B \beta^2 a^2}{4\pi^2} \int_1 \int_{BZ} f[E(\mathbf{k})] \{1 - f[E(\mathbf{k})]\} \times \left[E^2(\mathbf{k}) + \beta E(\mathbf{k}) \frac{dE(\mathbf{k})}{d\beta} \right] dk_x dk_y, \quad (15)$$

where $\beta = 1/(k_B T)$ and $f(E)$ is the Fermi–Dirac distribution. The specific heat of the normal state can be obtained by taking $\Delta(\mathbf{k})$ equal to zero in Eqs. (13) and (15). In Fig. 4, the calculated C_{el} (open triangles) for the sample with $x = 0.15$ using the parameters of Table 1 is shown and compared with the available experimental C_{el} data obtained from a sample of $\text{La}_{2-x}\text{Sr}_x\text{CuO}_4$ with a close doping level of $x = 0.14$ [17]. Notice that the theoretical results reveal an almost second-degree power-law behavior, in agreement with the experimental data, because the low-temperature behavior of C_{el} is sensitive to the existence of nodes in the gap. However, there is a difference between the theoretical and experimental data about the location and magnitude of the maximum C_{el} . The former could be due to the sample used for the theoretical calculation has a T_c of 41 K for $x = 0.15$, in contrast to the T_c of 37 K obtained from the sample of $x = 0.14$ [17]. The latter might be related to the limitation of our two-dimensional single-band electronic model, instead of a three-dimensional all electron model. In spite of its simplicity, the linear behavior of C_{el} in the normal state and the discontinuity between the normal and superconducting C_{el} are well reproduced.

The inset of Fig. 4 presents the first-Brillouin zone scheme of the single excitation energy gap (open triangles) defined as the minimal value of $E(\phi)$ along $\phi \equiv \tan^{-1}(k_y/k_x)$ direction. The projection of $E_{\min}(\phi)$ (green line) on the first-Brillouin zone corresponds to the Fermi surface, shown in Fig. 1(c). Observe that $E_{\min}(\phi)$ has a d -wave form with a maximum value of 7.12 meV, which is close to 8.5 meV reported by D.L. Feng et al. [18], 8.6 meV by A. Ino et al. [19], and 13.8 meV by M. Shi et al. [20]. Furthermore, the ratio of the single-excitation energy gap at the antinodal direction, for example at $\phi = 0$, over $k_B T_c$ is 2.015, which is larger than 1.764 from the BCS theory [16].

6. Conclusions

We have presented a generalized Hubbard model, whose parameters were determined by ARPES data for samples of

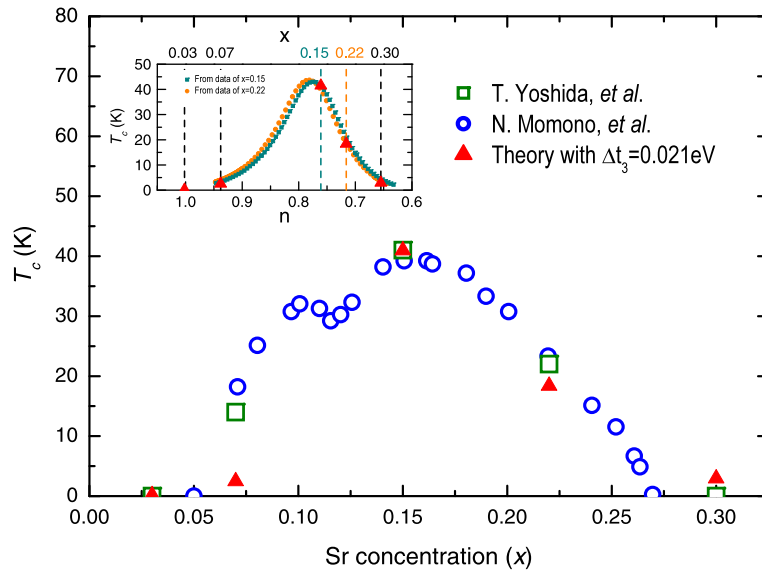


Fig. 3. (Color online.) Theoretical (solid triangles) critical temperature (T_c) as a function of the Sr concentration (x) in comparison with experimental data of T. Yoshida et al. (open squares) [12] and N. Momono et al. (open circles) [15]. Inset: T_c versus n for the Hamiltonian parameters obtained from $x = 0.15$ (solid squares) and $x = 0.22$ (solid circles) with the values of x indicated by dashed lines.

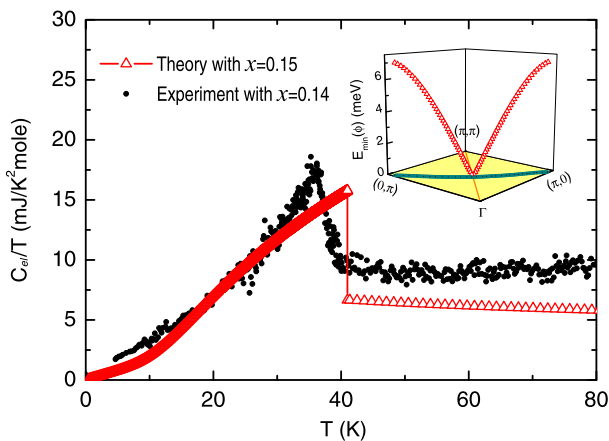


Fig. 4. (Color online.) Theoretical (open triangles) d -wave electronic specific heat (C_{el}) versus temperature (T) for $\text{La}_{2-x}\text{Sr}_x\text{CuO}_4$ with $x = 0.15$ in comparison with the experimental one (solid circles) for $x = 0.14$ [17]. Inset: Single excitation energy gap (open triangles) in the first Brillouin zone.

$\text{La}_{2-x}\text{Sr}_x\text{CuO}_4$ with different values of x . The electronic specific heat calculated without adjustable parameters is compared to experimental data and a good agreement is observed. It is worth mentioning that a single-band Hubbard model seems to be enough to reproduce the experimental dispersion relation and the second-neighbor correlated hopping could lead to a d -wave superconducting ground state with adequate values of T_c . Furthermore, this model predicts the observed diminution of the electronic density (n) from half-filling ($n = 1$) when x increases. Finally, the van Hove singularity seems to determine n with maximum T_c , as found in other models previously studied [21,22].

The present approach can be applied to other compounds including spin triplet superconductors [23]. Also, this study could be extended to include the effects of external perturbations, such as magnetic fields, on the physical properties of anisotropic su-

perconductors, by using the Bogoliubov–de Gennes formalism. This extension is currently being developed [24].

Acknowledgements

This work has been partially supported by CONACyT-131596, UNAM-IN102511, UNAM-IN107411. Computations have been performed at Bakliz and KanBalam of DGTIC, UNAM.

References

- [1] J. Bardeen, L.N. Cooper, J.R. Schrieffer, Phys. Rev. 108 (1957) 1175.
- [2] D.A. Wollman, et al., Phys. Rev. Lett. 71 (1993) 2134.
- [3] C.C. Tsuei, J.R. Kirtley, Rev. Mod. Phys. 72 (2000) 969.
- [4] E. Dagotto, Rev. Mod. Phys. 66 (1994) 763.
- [5] H.-B. Schüttler, A.J. Fedro, Phys. Rev. B 45 (1992) 7588.
- [6] L.A. Pérez, C. Wang, Solid State Commun. 121 (2002) 669.
- [7] Z.-H. Pan, et al., Phys. Rev. B 79 (2009) 092507(4).
- [8] H. Ding, et al., J. Phys.: Condens. Matter 23 (2011) 135701(6).
- [9] R.-H. He, et al., Science 331 (2011) 1579.
- [10] E. Dagotto, et al., Phys. Rev. B 49 (1994) 3548.
- [11] A. Damascelli, Z. Hussain, Z.-X. Shen, Rev. Mod. Phys. 75 (2003) 473.
- [12] T. Yoshida, et al., Phys. Rev. B 74 (2006) 224510.
- [13] E.N. Economou, Green's Functions in Quantum Physics, third ed., Springer, Berlin, 2006.
- [14] J.E. Hirsch, F. Marsiglio, Phys. Rev. B 39 (1989) 11515.
- [15] N. Momono, et al., Physica C 233 (1994) 395.
- [16] M. Tinkham, Introduction to Superconductivity, second ed., McGraw-Hill, New York, 1996.
- [17] T. Matsuzaki, N. Momono, M. Oda, M. Ido, J. Phys. Soc. Jpn. 73 (2004) 2232.
- [18] D.L. Feng, et al., Phys. Rev. Lett. 88 (2002) 107001(4).
- [19] A. Ino, et al., Phys. Rev. B 65 (2002) 094504(11).
- [20] M. Shi, et al., Phys. Rev. Lett. 101 (2008) 047002(4).
- [21] J.E. Hirsch, D.J. Scalapino, Phys. Rev. Lett. 56 (1986) 2732.
- [22] R.S. Markiewicz, J. Phys. Chem. Solids 58 (1997) 1179.
- [23] L.A. Pérez, J.S. Millán, C. Wang, Int. J. Mod. Phys. B 24 (2010) 5229.
- [24] C.G. Galván, L.A. Pérez, C. Wang, Bogoliubov–de Gennes analysis of d -wave superconductors through an ARPES-parameterized Hubbard model, in: The 26th International Conference on Low Temperature Physics, Beijing, China, 2011, Abstract 15P-B004.